High performance adsorption of hazardous triphenylmethane dye-crystal violet onto calcinated waste mussel shells

Sahra Dandil, Deniz Akin Sahbaz and Caglayan Acikgoz

ABSTRACT

Synthetic dyes are harmful to human beings, and the removal of colour from process or waste effluents is environmentally important. Crystal violet (CV) is a typical triphenylmethane dye, which is widely used in textile dyeing and paper printing industries. The present study shows that granulated and calcinated waste mussell shells (CWMS) can be used as a potential low-cost and locally available adsorbent for the removal of CV from aqueous solutions. The adsorption capacities of the CWMS for CV were investigated with respect to the effect of pH value, adsorbent dosage, contact time, initial dye concentration and temperature. Process variables were optimized, and a maximum dye adsorption of 482.0 mg/g was achieved at pH 6, 0.2 g/L adsorbent dosage, 220 min contact time and 25 °C for dye initial concentration of 100 mg/L. Adsorption kinetics and isotherms were followed by the pseudo-second order model and Freundlich isotherm models, respectively. Thermodynamic parameters demonstrated that adsorption of CV was spontaneous and endothermic in nature. The results indicated that the CWMS as a new adsorbent had the potential to serve in wastewater treatment applications, especially in the removal of CV from aqueous solutions.

Key words | adsorption, calcination, crystal violet, kinetics, mussel shells

Sahra Dandil
Caglayan Acikgoz
Department of Chemical Engineering,
Bilecik Seyh Edebali University,
11230, Bilecik,
Turkey

Deniz Akin Sahbaz (corresponding author)
Department of Chemical Engineering,
Afyon Kocatepe University,
03200, Afyonkarahisar,
Turkey
E-mail: *denizakin@aku.edu.tr*

INTRODUCTION

In recent years, as a result of the rapid increase of industrialization and urbanization, environmental problems such as water and air pollution have become a big problem in the world. One of these environmental problems is dyes present in the effluent of industrial plants. Most of the synthetic dyes used for colouring in different areas of industry such as textiles, paper and printing result in great damage to both the environment and living organisms (Sabna *et al.* 2016). In the dye industry, colour is described as the primary contaminant in the wastewater. Even though the concentration of a few dyes in effluent is less than 1 ppm, they are undesirable, toxic and carcinogenic pollutants (Gopi *et al.* 2016). Moreover, they are a hazard to aquatic life. As a cationic dye, crystal violet (CV) is one of the most used colouring agents in different industrial treatments. This dye is harmful for the living organisms exposed to it. Taking CV into the human body via respiration and the skin causes harmful diseases such as cancer and skin irritation (Mittal *et al.* 2010).

Mussel shells are found in different colours and shapes depending on where the mussels live. For this reason, there are many different species. When the shell characteristics of the mussel shells are examined, it is seen that there are many different layers from the inside to the outside (Bellotto & Miekeley 2007). It is known that the shell structure is rich in calcium mineral. Mussel shells are a major source of waste in some marine countries around the world. As a result of some studies on waste assessment, it has been determined that mussel shells can be effectively evaluated in different areas (Paradelo *et al.* 2016).

doi: 10.2166/wqrj.2019.050

Different techniques and methods have been used to remove contaminants in wastewater including chemical, physical and biological treatments; however, these techniques have several disadvantages such as high requirements regarding equipment and energy. The adsorption technique has proven to be efficient at removing contaminants from wastewater. Many different materials and low-cost waste can be used in the adsorption process. A recent study has shown that mussel shell is efficient at adsorbing heavy metal and other pollutants (Pena-Rodriguez *et al.* 2013; Ramirez-Perez *et al.* 2013; Seco-Reigosa *et al.* 2013; El Haddad *et al.* 2014; Fernandez-Calvino *et al.* 2014; Garrido-Rodriguez *et al.* 2014; Paradelo *et al.* 2016).

The present study focused on the removal of CV dye molecules from aqueous solutions by adsorption on calcinated waste mussel shell (CWMS). The effects of pH, adsorbent dosage, initial dye concentration, temperature and contact time on the adsorption of the CV dye onto the CWMS were investigated. The experimental data were applied to the Langmuir and Freundlich models. Furthermore, kinetic studies of the adsorption were carried out using pseudo-first order, pseudo-second order kinetic models and the intraparticle diffusion model.

MATERIALS AND METHODS

CWMS and its characterization

The mussel shell calcination process was carried out as previously described by El Haddad *et al.* (2014). Mussel shells are waste obtained from the seafood processing industry in Bilecik, Turkey. CV supplied by Fluka was used as adsorbate (the structure is given in Figure 1).

Waste mussel shells were washed with tap and distilled water, respectively, and dried in an oven for about 24 h until all the water had disappeared. After a drying process, waste mussel shells were crushed into small particles. Powdered mussel shells were calcinated at 900 °C for 2 h with a heating rate of 5 °C/min. The calcinated residue was washed with distilled water and dried at 80 °C. This sample was powdered again, then washed several times with distilled water, and dried at 105 °C. A second calcination treatment was performed at 400 °C for 4 h with a heating rate of 2 °C/min.

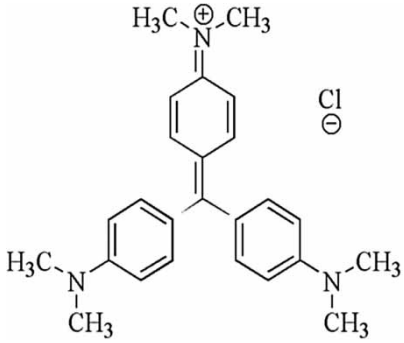

Figure 1 | Structure of CV.

The surface morphology of the CWMS was observed with a scanning electron microscope (SEM, Bruker, Germany). To analyse the carbon, oxygen and calcium element content of the CWMS, elementary characterization was carried out using an energy-dispersive spectroscopy (EDS, Bruker, Germany). The surface area of the CWMS was measured using a Micromeritics (ASAP 2020) BET (Brunauer, Emmett and Teller) instrument. The microstructure of the sorbent was characterized using physical adsorption/desorption of nitrogen at 77 K. Zeta potential measurements were carried out with a zeta potentiometer (Malvern Nano-ZS).

Batch experimental programme

The batch experimental adsorption studies were performed with 50 mL of dye solution with the known concentration, pH and adsorbent dosage in 100 mL Erlenmayer flasks. The flasks were agitated in a temperature controlled shaker (Termal H11960) at a constant speed of 120 rpm. Parameters affecting the adsorption process such as pH (4–11), adorbent dosage (0.2–2.0 g/L), initial dye concentration (20–100 mg/L), contact time (up to 60 min) and temperature (25–55 °C) were studied in a batch system. Every 5 minutes, flasks were withdrawn from the shaker and the remaining dye concentrations were analysed using a UV-Visible spectrophotometer (Agilent Cary 60 UV-Vis). The UV-Vis spectrophotometer, which uses the relationship between absorbance and wavelength, was used to determine dye concentrations. Absorbance measurements of standard solution were performed at 200–800 nanometer wavelength range. An absorbance–wavelength plot was obtained from this scanning. According to the plot, the maximum absorbance for CV was determined as 590 nm.

All experiments were carried out in triplicate. The experimental data were reported by averaging these three measurements.

The amount of the dye adsorbed per unit mass of the adsorbent (q_e, mg/g) and the percentage removal of the dye were calculated using the following equations:

$$q_e = \frac{V(C_0 - C_e)}{m} \quad (1)$$

$$Removal(\%) = \frac{C_0 - C_e}{C_0} \times 100 \quad (2)$$

where C_e (mg/L) is the concentration of CV aqueous solution at the equilibrium state, C_o (mg/L) is the initial concentration of CV in aqueous solution, V is the volume of the dye solution (L) used in the experiments, amd m is the weight of the CWMS adsorbent (g).

RESULTS AND DISCUSSION

Characterization

The surface characteristics affect the adsorption efficiency of the adsorbents. The surface morphology of the CWMS adsorbent was characterized using SEM. As can be seen from the enlarged view of Figure 2, the surface of the CWMS appears as spherical particles and their sizes are approximately 2 μm. Moreover, the figure shows that the shell surface is not homogeneous, with the existence of irregular forms.

Elemental analysis by EDS in point mode was conducted at the surface of the CWMS. It was determined that the CWMS contained significant amounts of calcium mineral. The mass fraction of calcium, carbon and oxygen were 41.12%, 4.84%, and 34.91%, respectively.

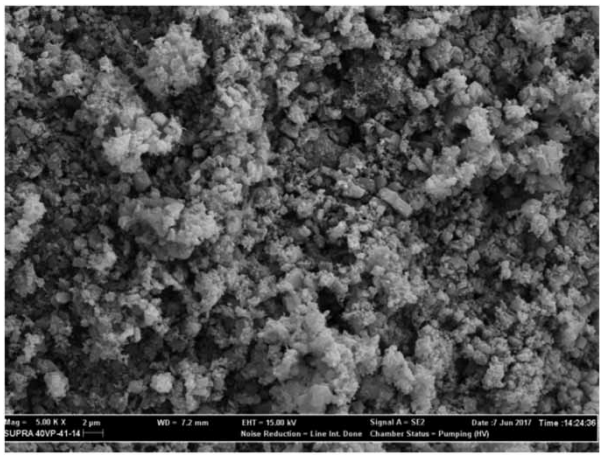

Figure 2 | SEM image of the CWMS.

The value of zeta potential is a measure of the interaction between particles. The charge densities of the surfaces depend on the amount of ions present on the surface. In adsorption experiments, the adsorption mechanism is between surfaces with different charge. Zeta potential is used to determine the charge of the surfaces. In the current study, the CWMS were analysed to determine their zeta potential value. From the obtained results, it was determined that shells had a negative zeta potential value. As a result, the shell could interact with positive charged surfaces.

N_2 adsorption measurement indicated that the BET surface area of the CWMS was 7.6139 m^2/g.

Effect of pH

The pH of the solution affects the surface charge on the adsorbent as well as on the adsorbates in the adsorption process. The effect of pH on the adsorption of the CV dye by the CWMS was studied by varying the initial pH of the dye solution from pH 4 to pH 11. The time required for adsorption to reach equilibrium was determined for each pH value. This part of the experimental studies was carried out by 2 g/L adsorbent dosage, 60 mg/L initial dye concentration at 25 °C. To determine adsorption capacities and removal efficiencies, the adsorption process was followed for 220 min at each pH value. At all experimental pH values, the adsorption capacities of the CWMS were about 28 ± 1 mg/g and removal efficiencies were approximately 95.67 ± 1%.

CV as a basic dye has a pKa value of 0.8 (Kumari *et al.* 2017). The adsorption process exhibited similar behaviour due to the low pKa value of the CV dye. The dye can be ionized at all experimental pH values and exists as a cationic species (Kumari *et al.* 2017). Thus, all the adsorption studies were carried out at pH 6 which is the natural pH of the dye solution.

Effect of adsorbent dosage

Adsorption dosage influences the adsorption process by affecting the adsorption capacity of the adsorbent. As seen in Figure 3, the adsorption capacity of the CWMS for the

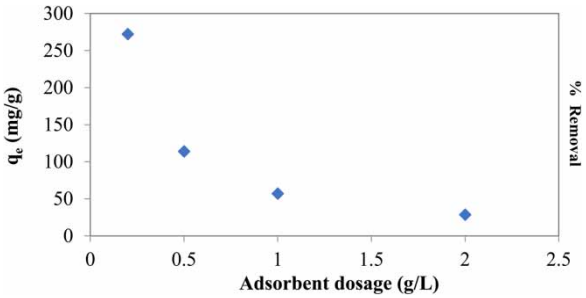

Figure 3 | The effect of adsorbent dosage on the CV dye adsorption by the CWMS (adsorption conditions: pH 6; initial dye concentration 60 mg/L; temperature 25 °C; contact time 220 min).

CV dye decreases from 272.2 mg/g to 28.6 mg/g when the adsorbent dosage increases from 0.2 g/L to 2 g/L. The decrease in adsorption capacity with increasing adsorbent dosage might be due to the aggregation of the adsorption sites by the adsorbent particles. The phenomenon leads to a decrease in total surface area of the particles required for the adsorption process (Ahmad & Mirza 2018).

Effect of initial dye concentration and contact time

Adsorption time is a very important factor in all adsorption processes. A quick uptake of contaminant and reaching equilibrium in a short time signifies the efficiency of the adsorbent. Figure 4 shows the effect of contact time on the adsorption of the CV dye onto the CWMS at various initial dye concentrations (20–100 mg/L). As shown in Figure 4, for all the initial concentrations, the adsorption amounts of the CV on the CWMS increase rapidly with an increase in time and

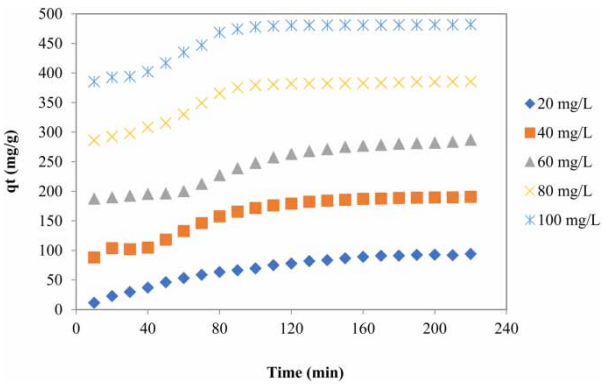

Figure 4 | The effect of contact time on the adsorption of the CV dye onto the CWMS (adsorption conditions: pH 6; adsorbent dosage 0.2 g/L; temperature 25 °C; initial dye concentration 20–100 mg/L).

then become slower until equilibrium is reached. The adsorption capacities of the CV reach maximum at 220 min.

Adsorption kinetic models

Three kinetic models, the Lagergren pseudo-first order, pseudo-second order and intraparticle diffusion models were chosen to explain the adsorption mechanism of the CV dye on the CWMS.

The Lagergren pseudo-first order model can be expressed as (Lagergren 1898):

$$log(q_e - q_t) = logq_e - \frac{k_1}{2.303}t \tag{3}$$

where k_1 (min^{-1}) is the pseudo-first order rate constant and t (min) is time. The values of k_1 and q_e were calculated from the slope and intercept of the linear plots obtained by graphical representation of $log\ (q_e - q_t)$ versus t (Figure 5(a)).

The pseudo-second order kinetic model can be represented in the following linear form (Ho & McKay 1999):

$$\frac{t}{q_t} = \frac{1}{k_2 q_e^2} + \frac{1}{q_e}t \tag{4}$$

where k_2 (g mg^{-1} min^{-1}) is the pseudo-second order rate constant of the adsorption. The values of q_e and k_2 were calculated from the slope and intercept of the linear plots obtained by graphical representation of t/q_t versus t (Figure 5(b)).

The intraparticle diffusion model can be expressed as follows (Weber & Morris 1963):

$$q_t = k_i t^{0.5} + c \tag{5}$$

where k_i is the intraparticle diffusion rate constant (mg g^{-1} $h^{-1/2}$) and c is a constant (mg g^{-1}). The plot of q_t versus $t_{0.5}$ should give the k_i and c values from the slope and intercept of the plot, respectively (Figure 5(c)).

The kinetic parameters and correlation coefficients (R^2) for the pseudo-first, pseudo-second order kinetic models and intraparticle diffusion model are summarized in Tables 1 and 2. As seen in these tables, the adsorption kinetic results follow the pseudo-second order model better than the other models which is indicated by higher R^2 values. Moreover,

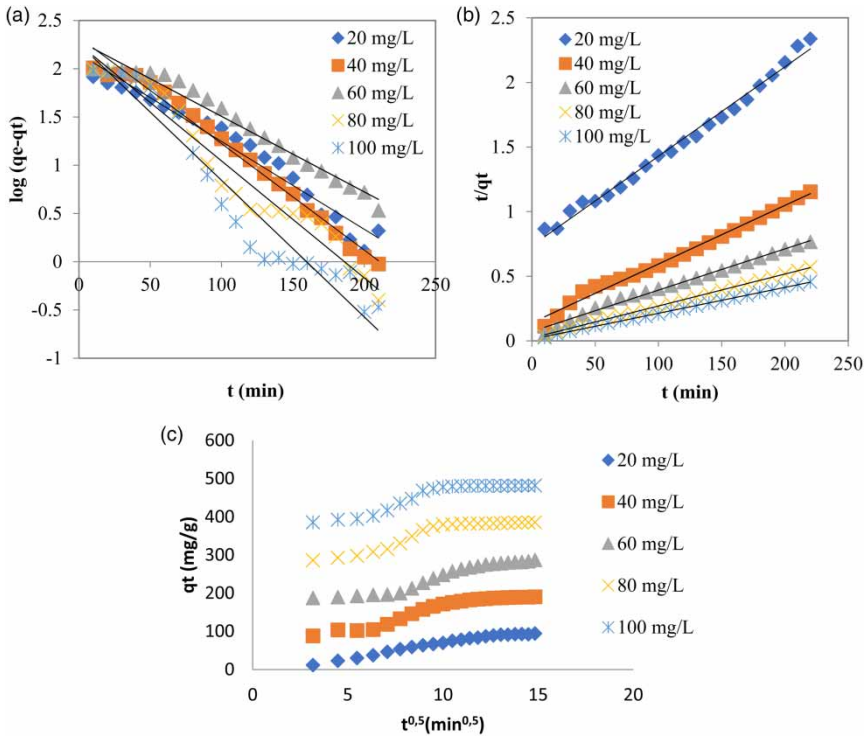

Figure 5 | Pseudo-first order (a) pseudo-second order (b) and intraparticle diffusion model (c) plots for the CV dye adsorption onto the CWMS.

the experimental values $q_{e,exp}$ are very similar to the values obtained in the pseudo-second order kinetic model $q_{e,cal}$ according to Table 1. This model shows that the removal of the CV dye from a solution by the CWMS is due to physicochemical interactions between the two phases (Ho & McKay 1999).

Adsorption isotherms

Adsorption isotherms are used to explain how the adsorbate molecules interact with adsorbent and attain equilibrium. In order to explore the adsorption mechanism of CV dye onto the CWMS, the Langmuir and Freundlich isotherm models were used in the current study.

The Langmuir isotherm is based on the assumption that adsorption takes place at specific equal sites within the adsorbent. The monolayer adsorption model suggests that an adsorbate molecule occupies a particular site and no further adsorption takes place at that site. The Langmuir isotherm can be presented in the following linear form (Langmuir 1918):

$$\frac{C_e}{q_e} = \frac{C_e}{q_{max}} + \frac{1}{q_{max} K_L} \tag{6}$$

Table 1 | Parameters of the Lagergren pseudo-first order and pseudo-second order models for adsorption of the CV dye onto the CWMS

		Lagergren first order kinetic model			Pseudo-second order kinetic model		
Initial CV concentration (mg/L)	$q_{e,exp}$ (mg/g)	$q_{e,cal}$ (mg/g)	k_1 (min^{-1})	R^2	$q_{e,cal}$ (mg/g)	k_2 ($g.mg^{-1}.min^{-1}$)	R^2
20	94.1	142.9	0.021	0.9600	144.9	6.090	0.9902
40	190.6	212.0	0.025	0.9855	222.2	0.144	0.9905
60	287.1	194.5	0.017	0.9673	312.5	0.139	0.9913
80	385.7	180.5	0.028	0.9587	400.0	0.279	0.9987
100	482.0	180.9	0.032	0.9370	500.0	0.315	0.9992

Table 2 | Parameters of the intraparticle diffusion model for adsorption of the CV dye onto the CWMS

	Intraparticle diffusion model								
Initial CV concentration (mg/L)	$k_{int,1}$ (mg g^{-1} min$^{-0.5}$)	C_1 (mg/g)	R_1^2	$k_{int,2}$ (mg g^{-1} min$^{-0.5}$)	C_2 (mg/g)	R_2^2	$k_{int,3}$ (mg g^{-1} min$^{-0.5}$)	C_3 (mg/g)	R_3^2
20	7.9453	−13.264	0.9953	8.6609	−15.277	0.9861	3.8478	38.511	0.8992
40	6.2845	70.62	0.7237	17.782	−5.4144	0.9864	2.6373	152.49	0.9116
60	2.1947	180.26	0.9831	16.334	82.206	0.9435	5.4856	205.77	0.9572
80	5.08	269.9	0.9995	19.838	180.79	0,9634	0.9972	370.65	0.9175
100	3.8135	374.08	0.9266	20.102	278.13	0.9586	0.3022	477.26	0.8879

where q_e and q_{max} (mg/g) are the equilibrium and maximum adsorption capacity, respectively. K_L (L/mg) is the Langmuir constant and C_e (mg/L) is the equilibrium concentration. The values of q_{max} and K_L were calculated from the slope and intercept of the linear plot C_e/q_e versus C_e (Figure 6(a)).

The Freundlich model assumes that the adsorption takes place on heterogeneous surfaces and the distribution of the heat on the adsorbent surface is nonuniform. The Freundlich isotherm can be expressed by the equation (Freundlich 1906; Freundlich & Heller 1939):

$$lnq_e = \left(\frac{1}{n}\right) lnC_e + lnK_F \tag{7}$$

where K_F and n are the Freundlich constants related to adsorption capacity and adsorption intensity, respectively. The values of n and K_F were calculated from the slope and intercept of the linear plot $ln\ q_e$ versus $ln\ C_e$ (Figure 6(b)).

The parameters for isotherm models of the CV dye adsorption onto the CWMS are listed in Table 3. The Freundlich isotherm model showed the best fit of the isotherm data with higher correlation coefficients (R^2), indicating that dye adsorbed onto the heterogeneous surface of the CWMS was a multilayer formation.

Effect of temperature and thermodynamic parameters

The effect of temperature on the CV adsorption of the CWMS was investigated using thermodynamic functions. Thermodynamic parameters such as free energy change (ΔG°), enthalpy change (ΔH°) and entropy change (ΔS°) were estimated using the following formulas (Liu & Lee 2014):

$$\Delta G^\circ = -RTlnK_C \tag{8}$$

$$\Delta G^\circ = \Delta H^\circ - T\Delta S^\circ \tag{9}$$

$$lnK_C = (\Delta S^\circ/R) - (\Delta H^\circ/RT) \tag{10}$$

$$K_C = q_e/C_e \tag{11}$$

The values of ΔH° and ΔS° were calculated from slope and intercept of the plot of $ln\ Kc$ against $1/T$. Table 4

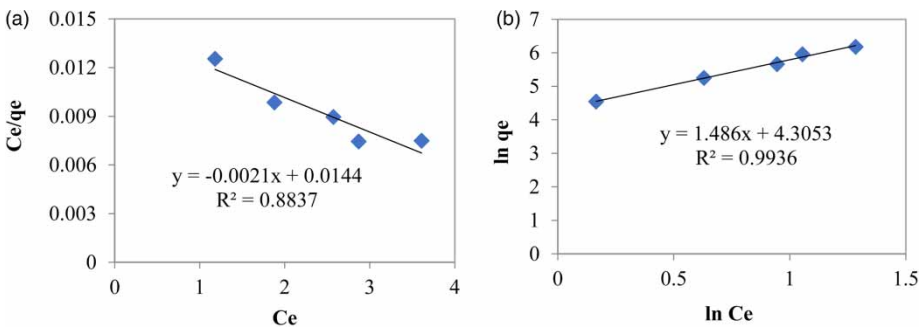

Figure 6 | Langmuir (a) and Freundlich (b) adsorption isotherms of the CV adsorption by the CWMS with initial dye concentration in the range of 20–100 mg/L (adsorption conditions: pH 6; adsorbent dosage 0.2 g/L; temperature 25 °C; contact time 220 min).

Table 3 | Adsorption isotherm constants for the adsorption of the CV dye onto the CWMS

Freundlich adsorption isotherm			Langmuir adsorption isotherm
K_F [mg/g (L/g)$^{1/n}$]	n	R^2	R^2
74.09	0.67	0.9936	0.8837

Table 4 | Thermodynamic parameters for adsorption of the CV dye onto the CWMS at different temperatures

T (K)	ΔG° (kJ.mol^{-1})	ΔH° (kJ.mol^{-1})	ΔS° (J.mol^{-1}.K^{-1})
298	−11.8	51.7	213.2
308	−13.9		
318	−16.1		
328	−18.2		

summarizes the thermodynamic parameters at different temperatures for the adsorption of the CV onto the CWMS. The obtained negative values of ΔG° at all temperatures reveal that the adsorption process is spontaneous. An increase in ΔG° values with increasing reaction temperatures can contribute to an increase in feasibility of adsorption at higher temperatures. The positive value of ΔH° indicates the endothermic nature of the adsorption process. The positive value of ΔS° suggests increased randomness of the solid–solution interface during the adsorption of CV ions onto the CWMS adsorbent.

Table 5 | Comparison of the adsorption capacities of various adsorbents for CV dye

Adsorbent	Adsorption capacity (mg/g)	Reference
CWMS	482.0	This study
Mango stone biocomposite	352.8	Shoukat *et al.* (2017)
Nanoparticle modified kaolin	247.7	Sun *et al.* (2017)
Fly ash based adsorbent material-supported zero-valent iron	172.4	Liu *et al.* (2018)
Surfactant modified magnetic nanoadsorbent	166.7	Muthukumaran *et al.* (2016)
Chitosan aniline composite	100.6	Tahir *et al.* (2017)
Ag nanoparticles immobilised on the activated carbon	87.2	AbdEl-Salam *et al.* (2017)
NaOH-modified rice husk	44.9	Chakraborty *et al.* (2011)

The data presented in Table 5 compare the adsorption capacities of various adsorbents for CV dye. The comparison shows that the CWMS have a higher adsorption capacity of CV than many of the other reported adsorbents. Furthermore, the CWMS as adsorbents are quite cheap materials. Thus, it can be stated that the CWMS are attractive and economical adsorbents which can be used for treatment of wastewater containing CV dye.

CONCLUSION

In the present study, the adsorptions of the CV dye onto the CWMS were studied by batch tests conducted under various experimental conditions, such as pH, contact time, initial dye concentrations and temperature. The optimum conditions maintained to remove the CV dye by the CWMS were: pH 6, adsorbent dosage 0.2 g/L, and temperature at 25 °C of 100 mg/L of the CV. The maximum adsorption capacity was found to be 482.0 mg/g. The pseudo-second order kinetic model and Langmuir isotherm model were found to describe the adsorption mechanism.

REFERENCES

AbdEl-Salam, A. H., Ewais, H. A. & Basaleh, A. S. 2017 Silver nanoparticles immobilised on the activated carbon as efficient adsorbent for removal of crystal violet dye from aqueous solutions. A kinetic study. *Journal of Molecular Liquids* **248**, 833–841. doi: 10.1016/j.molliq.2017.10.109.

Ahmad, R. & Mirza, A. 2018 Synthesis of Guar gum/bentonite a novel bionanocomposite: isotherms, kinetics and thermodynamic studies for the removal of Pb (II) and crystal violet dye. *Journal of Molecular Liquids* **249**, 805–814. doi: 10.1016/j.molliq.2017.11.082.

Bellotto, V. R. & Miekeley, N. 2007 Trace metals in mussel shells and corresponding soft tissue samples: a validation experiment for the use of *Perna perna* shells in pollution monitoring. *Analytical and Bioanalytical Chemistry* **389**, 769–776. doi: 10.1007/s00216-007-1420-y.

Chakraborty, S., Chowdhury, S. & Das Saha, P. 2011 Adsorption of crystal violet from aqueous solution onto NaOH-modified rice husk. *Carbohydrate Polymers* **86**, 1533–1541. doi: 10.1016/j.carbpol.2011.06.058.

El Haddad, M., Regti, A., Laamari, M. R., Slimani, R., Mamouni, R., Antri, S. E. & Lazar, S. 2014 Calcined mussel shells as a new and eco-friendly biosorbent to remove textile dyes from aqueous solutions. *Journal of the Taiwan Institute of*

Chemical Engineers **45**, 533–540. doi: 10.1016/j.jtice.2013.05.002.

Fernandez-Calvino, D., Garrido-Rodríguez, B., Cutillas-Barreiro, L., Araújo-Nespereira, P., Arias-Estévez, M., Fernández-Sanjurjo, M. J., Álvarez-Rodríguez, E. & Núñez-Delgado, A. 2014 Influence of mussel shell on As and Cr competitive and non-competitive sorption–desorption kinetics in a mine soil: stirred flowchamber experiments. *Geoderma* **232**, 300–308. doi: 10.1016/j.geoderma.2014.05.014.

Freundlich, H. M. F. 1906 Over the adsorption in solution. *The Journal of Physical Chemistry* **57**, 385–471.

Freundlich, H. & Heller, W. 1939 The adsorption of cis- and trans-azobenzene. *Journal of the American Chemical Society* **61**, 2228–2230. doi: 10.1021/ja01877a071.

Garrido-Rodriguez, B., Cutillas-Barreiro, L., Fernandez-Calvino, D., Arias-Estevez, M., Fernandez-Sanjurjo, M. J., Alvarez-Rodriguez, E. & Nunez-Delgado, A. 2014 Competitive adsorption and transport of Cd, Cu, Ni and Zn in a mine soil amended with mussel shell. *Chemosphere* **107**, 379–385. doi: 10.1016/j.chemosphere.2013.12.097.

Gopi, S., Pius, A. & Thomas, S. 2016 Enhanced adsorption of crystal violet by synthesized and characterized chitin nano whiskers from shrimp shell. *Journal of Water Process Engineering* **14**, 1–8. doi: 10.1016/j.jwpe.2016.07.010.

Ho, Y. S. & McKay, G. 1999 Pseudo-second order model for sorption processes. *Process Biochemistry* **34**, 451–465. doi: 10.1016/S0032-9592(98)00112-5.

Kumari, H. J., Krishnamoorthy, P., Arumugam, T. K., Radhakrishnan, S. & Vasudevan, D. 2017 An efficient removal of crystal violet dye from waste water by adsorption onto TLAC/Chitosan composite: a novel low cost adsorbent. *International Journal of Biological Macromolecules* **96**, 324–333. doi: 10.1016/j.ijbiomac.2016.11.077.

Lagergren, S. 1898 Zur theorie der sogenannten adsorption geloster stoffe (About the theory of so-called adsorption of soluble substances). *Kungliga Svenska Vetenskapsakademiens, Handlingar* **24** (4), 1–39.

Langmuir, I. 1918 The adsorption of gases on plane surfaces of glass, mica and platinum. *Journal of the American Chemical Society* **40**, 1361–1403. doi: 10.1021/ja02242a004.

Liu, X. & Lee, D. J. 2014 Thermodynamic parameters for adsorption equilibrium of heavy metals and dyes from wastewaters. *Bioresource Technology* **160**, 24–31. doi: 10.1016/j.biortech.2013.12.053.

Liu, J., Wang, Y., Fang, Y., Mwamulima, T., Song, S. & Peng, C. 2018 Removal of crystal violet and methylene blue from aqueous solutions using the fly ash-based adsorbent material-supported zero-valent iron. *Journal of Molecular Liquids* **250**, 468–476. doi: 10.1016/j.molliq.2017.12.003.

Mittal, A., Mittal, J., Malviya, A., Kaur, D. & Gupta, V. K. 2010 Adsorption of hazardous dye crystal violet from wastewater by waste materials. *Journal of Colloid and Interface Science* **343** (2), 463–473. doi: 10.1016/j.jcis.2009.11.060.

Muthukumaran, C., Sivakumar, V. M. & Thirumarimurugan, M. 2016 Adsorption isotherms and kinetic studies of crystal violet dye removal from aqueous solution using surfactant modified magnetic nanoadsorbent. *Journal of the Taiwan Institute of Chemical Engineers* **63**, 354–362. doi: 10.1016/j.jtice.2016.03.034.

Paradelo, R., Conde-Cid, M., Cutillas-Barreiro, L., Arias-Estevez, M., Nóvoa-Munoz, J. C., Álvarez-Rodríguez, E., Fernández-Sanjurjo, M. J. & Núnez-Delgado, A. 2016 Phosphorus removal from wastewater using mussel shell: investigation on retention mechanisms. *Ecological Engineering* **97**, 558–566. doi: 10.1016/j.ecoleng.2016.10.066.

Pena-Rodriguez, S., Bermudez-Couso, A., Novoa-Munoz, J. C., Arias-Estevez, M., Fernandez-Sanjurjo, M. J., Alvarez-Rodriguez, E. & Nunez-Delgado, A. 2013 Mercury removal using ground and calcined mussel shell. *Journal of Environmental Sciences* **25**, 2476–2486. doi: 10.1016/S1001-0742(12)60320-9.

Ramirez-Perez, A. M., Paradelo, M., Nóvoa-Munoz, J. C., Arias-Estévez, M., Fernández-Sanjurjo, M. J., Álvarez-Rodríguez, E. & Núñez-Delgado, A. 2013 Heavy metal retention in copper mine soil treated with mussel shells: batch and column experiments. *Journal of Hazardous Materials* **248**, 122–130. doi: 10.1016/j.jhazmat.2012.12.045.

Sabna, V., Thampi, S. G. & Chandrakaran, S. 2016 Adsorption of crystal violet onto functionalised multi-walled carbon nanotubes: equilibrium and kinetic studies. *Ecotoxicology and Environmental Safety* **134**, 390–397. doi: 10.1016/j.ecoenv.2015.09.018.

Seco-Reigosa, N., Peña-Rodríguez, S., Nóvoa-Muñoz, J. C., Arias-Estévez, M., Fernández-Sanjurjo, M. J., Álvarez-Rodríguez, E. & Núñez-Delgado, A. 2013 Arsenic, chromium and mercury removal using mussel shell ash or a sludge/ashes waste mixture. *Environmental Science and Pollution Research* **20**, 2670–2678. doi: 10.1007/s11356-012-1192-6.

Shoukat, S., Bhatti, H. N., Iqbal, M. & Noreen, S. 2017 Mango stone biocomposite preparation and application for crystal violet adsorption: a mechanistic study. *Microporous and Mesoporous Materials* **239**, 180–189. doi: 10.1016/j.micromeso.2016.10.004.

Sun, P., Hui, C., Khan, R. A., Guo, X., Yang, S. & Zhao, Y. 2017 Mechanistic links between magnetic nanoparticles and recovery potential and enhanced capacity for crystal violet of nanoparticles-coated kaolin. *Journal of Cleaner Production* **164**, 695–702. doi: 10.1016/j.jclepro.2017.07.004.

Tahir, N., Bhatti, H. N., Iqbal, M. & Noreen, S. 2017 Biopolymers composites with peanut hull waste biomass and application for crystal violet adsorption. *International Journal of Biological Macromolecules* **94**, 210–220. doi: 10.1016/j.ijbiomac.2016.10.013.

Weber, W. J. & Morris, J. C. 1963 Kinetics of adsorption on carbon from solution. *Journal of the Sanitary Engineering Division* **89**, 31–60.

First received 22 October 2018; accepted in revised form 26 January 2019. Available online 1 March 2019